SIAM J. NUMER. ANAL.
Vol. 40, No. 1, pp. 376–401

NUMERICAL TREATMENT OF DEFECTIVE BOUNDARY CONDITIONS FOR THE NAVIER–STOKES EQUATIONS*

L. FORMAGGIA†, J.-F. GERBEAU‡, F. NOBILE‡, AND A. QUARTERONI†§

Abstract. We present a formulation for accommodating defective boundary conditions for the incompressible Navier–Stokes equations where only averaged values are prescribed on measurable portions of the boundary. In particular we consider the case where the flow rate is imposed on several domain sections. This methodology has an interesting application in the numerical simulation of flow in blood vessels, when only a reduced set of boundary data are generally available for the upstream and downstream sections.

Key words. Navier–Stokes equations, boundary conditions, finite elements, Lagrange multipliers, fractional step methods, simulation of blood flow

AMS subject classifications. 35Q30, 65N30

PII. S003614290038296X

Introduction. A necessary condition for the existence of the solution of the incompressible Navier–Stokes equations on a bounded domain Ω is that an appropriate set of boundary conditions is imposed on $\partial\Omega$. In a classical setting, at each point on the boundary one needs a number of conditions equal to the spatial dimension of the problem. Typically, one can prescribe the components of the velocity (Dirichlet boundary condition) or those of the Cauchy normal stress (Neumann boundary condition) or an appropriate combination of velocity and normal stress.

In this work, we will consider the specific situation occurring when one has at their disposal only averaged quantities on portions of the domain boundary, a priori insufficient to "close" the differential problem at hand. We will refer to this incomplete set as *defective* boundary conditions. An important applicative field where this situation occurs is the numerical simulation of blood flow in the human vascular system. If we aim at computing the blood flow field in an isolated portion of an artery—for instance, reconstructed from medical images—we immediately face the problem of which boundary conditions to impose at the artificial upstream and downstream sections. A possibility is to exploit data coming from measurements. Yet the most common techniques are normally able to measure only flow rates or average pressures and not complete fields as would be required for the numerical computations.

A similar situation occurs when one wants to simulate the cardiovascular system by multiscale approaches such those proposed in [8] and [6]. In that case, the boundary data for the Navier–Stokes equations do not come from measurements, but rather come as the output of simplified models of the global cardiovascular system.

*Received by the editors December 22, 2000; accepted for publication (in revised form) October 26, 2001; published electronically May 10, 2002. The work has been partially supported by the Swiss National Science Foundation project 21-54139.98, by MURST Cofin. 1998 "Advanced Numerical Methods for Scientific Computing," and by the special project of the Politecnico di Milano "Multiscale Computing in Biofluidynamics."

http://www.siam.org/journals/sinum/40-1/38296.html

†Département de Mathématiques, École Polytechnique Fédérale de Lausanne, CH-1015, Lausane, Switzerland (luca.formaggia@epfl.ch, fabio.nobile@epfl.ch, alfio.quarteroni@epfl.ch).

‡INRIA, Projet M3N, Rocquencourt B.P. 105, F-78153 Le Chesnay Cedex, France (Jean-Frederic.Gerbeau@inria.fr).

§Dipartimento di Matematica "Francesco Brioschi," Politecnico di Milano, Piazza Leonardo da Vinci 32, I-20133 Milano, Italy.

These simple models, which are typically based on the solution of either a system of ordinary differential equations or of one-dimensional differential problems, normally provide the evolution of mean pressure and velocity inside the various regions of the cardiovascular system. If we want to use them to feed boundary data into a more detailed local model based on the solution of the Navier–Stokes equations, we need to have a way to "translate" these mean quantities in mathematically sound boundary conditions for the Navier–Stokes problem. This issue has been addressed in the cited references. Another interesting application of the technique proposed in this work is in the simulation of a free interface problem, when one wants to ensure that the numerical approximation satisfies mass conservation within machine precision. An example of a problem of this type is presented in the section dedicated to numerical experiments. Another applicative field is the simulation of flow in pipes, when measuring sensors provide only flow rate information.

A viable approach to handle the case of defective boundary conditions is provided by the so-called *do-nothing* boundary conditions proposed in [10].

In this paper we analyze another, somewhat more flexible, alternative based on the use of Lagrange multipliers. In particular, we will consider the case when given flow rates Q_i are to be prescribed on several sections of the domain boundary. The corresponding variational formulation, augmented by the Lagrange multipliers, is presented in all generality and analyzed for the case of a Stokes problem, where a well-posedness result is given. We present several approaches for the numerical solution of this problem in the context of fractional step schemes and compare their properties with respect to the effective fulfillment of the imposed flow rate constraint and computational efficiency. Several numerical experiments prove the effectiveness of this technique, which may be implemented in existing software with little efforts. This is an advantage with respect to the do-nothing approach, whose implementation for the prescribed flow rate problem is not straightforward, as it would require the construction of suitable (nonstandard) test functions.

We also discuss how to impose an average pressure (or normal stresses) on measurable parts of the domain. We show how the Lagrange multiplier technique may be successfully implemented in the case of slip boundary conditions for the velocity.

The technique developed here is targeted to applications where it is important to match the solution at the inflow and/or the outflow with known average data. In the present form it is not directly applicable for far-field conditions in unbounded domains and in particular for devising "nonabsorbing" boundary treatment for vortex flow. The reader interested in this particular aspect may, for instance, refer to [3, 4, 5].

In the first section of this work we address the problem in general terms and we introduce the functional setting for the analysis. We also give an overview of the do-nothing approach applied to problems where either the flow rate or the average normal stress is imposed on a portion of the computational domain boundary. In section 2 we introduce the alternative formulation given by a Lagrange multiplier approach and carry out its analysis. In section 3 we propose several algorithms that are suitable for its implementation in the context of the solution of the Navier–Stokes equations by algebraic fractional step techniques. Finally, section 4 presents numerical results illustrating the effectiveness of the proposed methodology.

1. Problem formulation and defective boundary conditions. Let Ω be a bounded domain of $\mathbb{R}^d$, $d = 2$ or 3, whose boundary $\partial\Omega$ is decomposed into the union of Γ and several disjoint sections $S_0, S_1, \ldots, S_n$, $n \geq 1$ (see Figure 1).

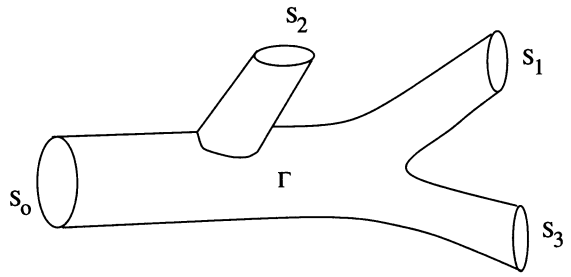

FIG. 1. *The partition of the boundary of the domain* Ω.

We are interested in solving the Navier–Stokes equations in Ω,

$$\begin{cases} \partial_t \mathbf{u} + \mathbf{u} \cdot \nabla \mathbf{u} + \nabla p - \nu \triangle \mathbf{u} = \mathbf{f}, & t > 0, \\ \operatorname{div} \mathbf{u} = 0, & t > 0, \\ \mathbf{u} = \mathbf{u}_0, & t = 0, \end{cases} \tag{1.1}$$

supplemented by homogeneous boundary conditions on Γ,

$$\mathbf{u}|_\Gamma = 0, \tag{1.2}$$

while two different kinds of boundary conditions will be considered on the sections S_i, $i = 0, \ldots, n$. Both are well suited for blood flow simulations [18, 6], where Ω would represent the portion of an artery, Γ the vessel wall, and S_i the artificial upstream and downstream sections. Even if for this specific problem the vessel wall should be considered moving with time because of the flexibility of the vessel wall structure, here we will address only the case where Γ is fixed.

The first condition we consider is the so-called *prescribed mean pressure problem* which requires that

$$\frac{1}{\operatorname{meas}(S_i)} \int_{S_i} p \, ds = P_i, \quad i = 0, \ldots, n, \tag{1.3}$$

where each P_i is a prescribed function of the time t, constant on S_i.

The second condition we wish to address is the *prescribed flow rate problem*

$$\int_{S_i} \mathbf{u} \cdot \mathbf{n} \, ds = Q_i \quad \text{for } i = 0, \ldots, n, \tag{1.4}$$

where the flow rates Q_i's (also called *velocity fluxes*) are assigned functions of time. Due to the fluid incompressibility fluid, a compatibility relation must exist among the fluxes Q_i, namely Q_0 must be equal to $-\sum_{i=1}^{n} Q_i$.

The initial-boundary value problem (1.1)–(1.2) with either (1.3) or (1.4) is not well-posed from a physical point of view, since its solution is not unique. Indeed, on every section S_i, we are prescribing just one scalar condition rather than d conditions at every point $\mathbf{x} \in S_i$, as it should be.

In [10] the do-nothing approach was advocated as a way of solving the two situations just presented. By this technique, a particular weak formulation is devised which allows to fulfill conditions (1.3) (resp., (1.4)) at some extent, giving rise to a well-posed problem. In fact, this formulation contains also "implicit" (Neumann-like) boundary conditions which select one particular solution among all the physical solutions of the original differential problem.

We will here give a brief presentation of this approach. Let us introduce the functional spaces

$$V = \left\{ \mathbf{v} \in \left[H^1(\Omega)\right]^d, \mathbf{v}|_\Gamma = 0 \right\} \qquad \text{and} \qquad M = L^2(\Omega).$$

We suppose that $\mathbf{f} \in V'$ and we introduce the functional $\phi_i \in V'$, $i = 0, \ldots, n$, which measures the flux of a vector function through the surface S_i. Precisely,

$$\langle \phi_i, \mathbf{v} \rangle = \int_{S_i} \mathbf{v} \cdot \mathbf{n}\, ds \quad \forall \mathbf{v} \in V,$$

where $\mathbf{n}$ is the outward unit normal vector on $\partial\Omega$. For this reason ϕ_i is called the *flux functional* on S_i.

Then, the do-nothing formulation for the *mean pressure problem* reads as follows: find $\mathbf{u} \in V$ and $p \in M$ such that, for all $\mathbf{v} \in V$ and $q \in M$,

$$\text{(1.5)} \qquad \begin{cases} (\partial_t \mathbf{u} + \mathbf{u} \cdot \nabla \mathbf{u}, \mathbf{v}) + \nu(\nabla \mathbf{u}, \nabla \mathbf{v}) - (p, \operatorname{div} \mathbf{v}) = \langle \mathbf{f}, \mathbf{v} \rangle - \displaystyle\sum_{i=0}^{n} P_i \langle \phi_i, \mathbf{v} \rangle, \\ (q, \operatorname{div} \mathbf{u}) = 0, \end{cases}$$

for all $t > 0$, with $\mathbf{u} = \mathbf{u}_0$ for $t = 0$.

It follows easily, by using the Green formula, that the solution of (1.5) satisfies

$$\left(p - \nu \frac{\partial u_n}{\partial \mathbf{n}} \right) \Big|_{S_i} = P_i, \qquad \frac{\partial \mathbf{u}_\tau}{\partial \mathbf{n}} \Big|_{S_i} = 0 \quad \text{for } i = 0, \ldots, n,$$

where we have set $u_n = \mathbf{u} \cdot \mathbf{n}$ and $\mathbf{u}_\tau = \mathbf{u} - u_n \mathbf{n}$.

Thus

$$\text{(1.6)} \qquad \frac{1}{\operatorname{meas}(S_i)} \int_{S_i} p\, ds = P_i + \frac{\nu}{\operatorname{meas}(S_i)} \int_{S_i} \frac{\partial u_n}{\partial \mathbf{n}}\, ds.$$

We conclude that the desired condition (1.3) is recovered exactly only in those cases where the last integral in (1.6) vanishes. This occurs, for instance, when S_i is a plane section perpendicular to a cylindrical pipe. Otherwise, P_i will be the mean value of the normal component of the normal stresses on S_i.

For the *prescribed flow rate problem*, the do-nothing approach is formulated as follows. Let us introduce the space

$$V^\star = \{ \mathbf{v} \in V, \langle \phi_i, \mathbf{v} \rangle = 0, i = 0, \ldots, n \}$$

and the vector functions $\mathbf{b}_i \in V$, $i = 1, \ldots, n$, (called *flux-carriers*) that satisfy

$$\operatorname{div} \mathbf{b}_i = 0, \quad \int_{S_0} \mathbf{b}_i \cdot \mathbf{n}\, ds = -1, \quad \int_{S_j} \mathbf{b}_i \cdot \mathbf{n}\, ds = \delta_{ij} \quad \text{for } i, j = 1, \ldots, n.$$

The weak formulation of problem (1.1), (1.2), (1.4) proposed in [10] reads as follows: Find $\mathbf{u} = \mathbf{w} + \sum_{i=1}^{n} Q_i \mathbf{b}_i$, with $\mathbf{w} \in V^\star$ and $p \in M \setminus \mathbb{R}$ such that for all $\mathbf{v} \in V^\star$ and $q \in M$

$$\text{(1.7)} \qquad \begin{cases} (\partial_t \mathbf{u} + \mathbf{u} \cdot \nabla \mathbf{u}, \mathbf{v}) + \nu(\nabla \mathbf{u}, \nabla \mathbf{v}) - (p, \operatorname{div} \mathbf{v}) = 0, \\ (q, \operatorname{div} \mathbf{u}) = 0 \end{cases}$$

for all $t > 0$, with $\mathbf{u} = \mathbf{u}_0$ for $t = 0$.

The corresponding solution satisfies

$$\left(p - \nu\frac{\partial u_n}{\partial \mathbf{n}}\right)|_{S_i} = P_i, \qquad \frac{\partial \mathbf{u}_\tau}{\partial \mathbf{n}}|_{S_i} = 0 \quad \text{for } i = 0, \dots, n, \tag{1.8}$$

where the P_i's are *a priori* unknown constants (in space).

The formulation of the *mean pressure problem* may be easily discretized as it can be regarded as a classical Navier–Stokes problem with Neumann boundary conditions. On the other hand, the definition of the functional space $V^\star$ makes the implementation of the *prescribed flow rate problem* less straightforward.

2. A Lagrange multiplier approach for flow rate boundary conditions. In this section, we propose a slightly different formulation of the prescribed flow rate problem presented above. We consider (1.1) and (1.2) and we prescribe the velocity flux on all but one section of $\partial\Omega$. More precisely, we aim at satisfying

$$\langle \phi_i, \mathbf{u}\rangle = \int_{S_i} \mathbf{u}\cdot\mathbf{n}\, ds = Q_i \quad \text{for } i = 1, \dots, n, \tag{2.1}$$

plus the following homogeneous Neumann boundary condition on S_0:

$$\left(-p\mathbf{n} + \frac{\partial \mathbf{u}}{\partial \mathbf{n}}\right)\Big|_{S_0} = 0. \tag{2.2}$$

The motivation of such an approach will be clarified in Remark 2.

Our goal is to formulate the initial-boundary value problem (1.1), (1.2), (2.1), (2.2) in a way that its numerical approximation be as simple as possible to implement. We look for $\mathbf{u} \in V$, $p \in M$, and $\lambda_1, \dots, \lambda_n \in \mathbb{R}$ such that, for all $\mathbf{v} \in V$ and $q \in M$,

$$\begin{cases} (\partial_t \mathbf{u} + \mathbf{u}\cdot\nabla\mathbf{u}, \mathbf{v}) + \nu(\nabla\mathbf{u}, \nabla\mathbf{v}) + \displaystyle\sum_{i=1}^{n} \lambda_i \langle \phi_i, \mathbf{v}\rangle - (p, \operatorname{div}\mathbf{v}) = \langle \mathbf{f}, \mathbf{v}\rangle, \\ (q, \operatorname{div}\mathbf{u}) = 0, \\ \langle \phi_i, \mathbf{u}\rangle = Q_i, \qquad i = 1, \dots, n, \end{cases} \tag{2.3}$$

for all $t > 0$, with $\mathbf{u} = \mathbf{u}_0$ for $t = 0$.

Note that now the test functions $\mathbf{v}$ are taken in V, a space which is more straightforward to discretize than $V^\star$.

PROPOSITION 2.1. *Any smooth solution of* (2.3) *satisfies the additional boundary conditions*

$$\left(p - \nu\frac{\partial u_n}{\partial \mathbf{n}}\right)|_{S_i} = \lambda_i \quad \textit{and} \quad \frac{\partial \mathbf{u}_\tau}{\partial \mathbf{n}}|_{S_i} = 0, \quad i = 1, \dots, n. \tag{2.4}$$

In particular, this yields that both $\frac{\partial \mathbf{u}_\tau}{\partial \mathbf{n}}$ *and* $p - \nu\frac{\partial u_n}{\partial \mathbf{n}}$ *are indeed constant over* S_i *for* $i = 1, \dots, n$. *Furthermore,* $(\mathbf{u}, p)$ *satisfies* (1.1), (1.2), (2.1), (2.2).

Proof. Conditions (1.2) and (2.1) are obviously satisfied. Integrating by parts the first equation of (2.3) yields for any $\mathbf{v} \in V$

$$\begin{aligned} \langle \partial_t \mathbf{u} + \mathbf{u}\cdot\nabla\mathbf{u} - \nu\triangle\mathbf{u} + \nabla p, \mathbf{v}\rangle + \int_{S_0} \left(\nu\frac{\partial \mathbf{u}}{\partial \mathbf{n}} - p\mathbf{n}\right)\cdot\mathbf{v}\, ds \\ + \sum_{i=1}^{n} \int_{S_i} \left(\nu\frac{\partial \mathbf{u}}{\partial \mathbf{n}} - p\mathbf{n} + \lambda_i\mathbf{n}\right)\cdot\mathbf{v}\, ds = \langle \mathbf{f}, \mathbf{v}\rangle. \end{aligned} \tag{2.5}$$

Now taking $\mathbf{v} \in \mathcal{D}(\Omega)$, we recover the momentum equation (1.1) in the sense of $\mathcal{D}'(\Omega)$. Consequently, from (2.5), it follows that

$$\int_{S_0} \left(\nu \frac{\partial \mathbf{u}}{\partial \mathbf{n}} - p\mathbf{n} \right) \cdot \mathbf{v}\, ds + \sum_{i=1}^{n} \int_{S_i} \left(\nu \frac{\partial \mathbf{u}}{\partial \mathbf{n}} - p\mathbf{n} + \lambda_i \mathbf{n} \right) \cdot \mathbf{v}\, ds = 0$$

for all $\mathbf{v} \in V$. Now using the splitting of the trace of u on $\partial\Omega$ in its normal and tangential component $\mathbf{u}|_{\partial\Omega} = u_n \mathbf{n} + \mathbf{u}_\tau$, we deduce relations (2.2) and (2.4). □

Remark 1. Among all possible solutions of (1.1), (1.2), (2.1), (2.2), problem (2.3) selects the one that satisfies the additional boundary condition (2.4).

Remark 2. In (2.3), we could have imposed a flux Q_0 on S_0, instead of the homogeneous Neumann condition (2.2). The corresponding problem would have been as follows: find $\mathbf{u} \in V$, $\tilde{p} \in M$, and $\tilde{\lambda}_0, \tilde{\lambda}_1, \ldots, \tilde{\lambda}_n \in \mathbb{R}$ such that, for all $\mathbf{v} \in V$ and $q \in M$,

$$\text{(2.6)} \qquad \begin{cases} (\partial_t \mathbf{u} + \mathbf{u} \cdot \nabla \mathbf{u}, \mathbf{v}) + \nu(\nabla \mathbf{u}, \nabla \mathbf{v}) + \displaystyle\sum_{i=0}^{n} \tilde{\lambda}_i \langle \phi_i, \mathbf{v} \rangle - (p, \operatorname{div} \mathbf{v}) = \langle \mathbf{f}, \mathbf{v} \rangle, \\ (q, \operatorname{div} \mathbf{u}) = 0, \\ \langle \phi_i, \mathbf{u} \rangle = Q_i, \qquad i = 0, \ldots, n, \end{cases}$$

for all $t > 0$, with $\mathbf{u} = \mathbf{u}_0$ for $t = 0$.

Due to the incompressibility of the fluid, the value of Q_0 must be equal to $-\sum_{i=1}^{n} Q_i$ (otherwise the problem has no solution). If $(\mathbf{u}, \tilde{p}, \tilde{\lambda}_0, \tilde{\lambda}_1, \ldots, \tilde{\lambda}_n)$ is a solution of (2.6), then, for any constant $C \in \mathbb{R}$, $(\mathbf{u}, \tilde{p} + C, \tilde{\lambda}_0 + C, \tilde{\lambda}_1 + C, \ldots, \tilde{\lambda}_n + C)$ is also a solution. The solution of (2.6) is thus defined up to an additive constant. Now, we set this constant C equal to $-\tilde{\lambda}_0$, and we denote $\tilde{p} + C$ and $\tilde{\lambda}_i + C$ by p and λ_i. Then, $(\mathbf{u}, p, \lambda_1, \ldots, \lambda_n)$ is the solution of (2.3) and, according to the "implicit" boundary condition (2.4), $\lambda_0 = 0$ yields simply the Neumann boundary condition (2.2). In other words, problem (2.3) (with the Neumann condition on S_0) and (2.6) (with the flux condition on S_0) are equivalent as soon as the "free" constant of problem (2.6) is well chosen.

Remark 3. From a theoretical viewpoint, our approach is very close to the do-nothing formulation recalled in the previous section. Comparing (1.8) and (2.4), we may note that the Lagrange multipliers corresponding to the constraints on the flux are in fact equal to the "a priori unknown" constants of the do-nothing formulation (1.8). Yet, our approach uses a standard functional space V which can be more straightforwardly discretized than the space V^*.

Now, for the sake of simplicity, we restrict ourselves to the analysis of the stationary Stokes problem (which embodies however all relevant difficulties of our Lagrange multiplier approach): find $(\mathbf{u}, p, \lambda_1, \ldots, \lambda_n) \in V \times M \times \mathbb{R}^n$ such that for all $(\mathbf{v}, q) \in V \times M$

$$\text{(2.7)} \qquad \begin{cases} \nu(\nabla \mathbf{u}, \nabla \mathbf{v}) + \displaystyle\sum_{i=1}^{n} \lambda_i \langle \phi_i, \mathbf{v} \rangle - (p, \operatorname{div} \mathbf{v}) = \langle \mathbf{f}, \mathbf{v} \rangle, \\ (q, \operatorname{div} \mathbf{u}) = 0, \\ \langle \phi_i, \mathbf{u} \rangle = Q_i, \ i = 1, \ldots, n. \end{cases}$$

The extension of the analysis to the complete time-dependent, nonlinear problem (2.3) can then be carried out by usual techniques (see, e.g., [20, 9, 19]).

PROPOSITION 2.2. *Problem* (2.7) *is well-posed.*

Proof. In order to prove existence, let us denote by $(\tilde{\mathbf{u}}, \tilde{p}) \in V \times M$ the solution of

$$\begin{cases} \nu(\nabla\tilde{\mathbf{u}}, \nabla\mathbf{v}) - (\tilde{p}, \operatorname{div}\mathbf{v}) = \langle \mathbf{f}, \mathbf{v}\rangle, \\ (q, \operatorname{div}\tilde{\mathbf{u}}) = 0 \end{cases} \tag{2.8}$$

for all $(\mathbf{v}, q) \in V \times M$. This is the weak formulation of the Stokes problem with homogeneous Dirichlet conditions on Γ and homogeneous Neumann conditions on $\partial\Omega \setminus \Gamma$.

Moreover, for $i = 1, \ldots, n$, let $(\mathbf{w}_i, \pi_i) \in V \times M$ be the solution of the problem

$$\begin{cases} \nu(\nabla\mathbf{w}_i, \nabla\mathbf{v}) - (\pi_i, \operatorname{div}\mathbf{v}) = -\langle \phi_i, \mathbf{v}\rangle, \\ (q, \operatorname{div}\mathbf{w}_i) = 0, \end{cases} \tag{2.9}$$

for all $(\mathbf{v}, q) \in V \times M$.

Both systems (2.8) and (2.9) admit a unique solution. Note that the equations satisfied by $(\tilde{\mathbf{u}}, \tilde{p})$ are the unconstrained counterpart of (2.7) and that the solution $(\mathbf{w}_i, \pi_i)$ of (2.9) depends only on the geometry and not on the data of the Stokes problem. In some sense, the functions $\mathbf{w}_i$ are related to the flux-carriers $\mathbf{b}_i$ introduced in the do-nothing formulation (1.7).

We set, then, $\mathbf{u} = \tilde{\mathbf{u}} + \sum_{i=1}^{n} \lambda_i \mathbf{w}_i$ and $p = \tilde{p} + \sum_{i=1}^{n} \lambda_i \pi_i$. No matter how the λ_i, $i = 1, \ldots, n$, are chosen, $(\mathbf{u}, p)$ satisfies the first two equations of (2.7). If we further require $\mathbf{u}$ to satisfy the third equation of (2.7), we obtain the following equations:

$$\langle \phi_i, \tilde{\mathbf{u}}\rangle + \sum_{j=1}^{n} \lambda_j \langle \phi_i, \mathbf{w}_j\rangle = Q_i, \quad i = 1, \ldots, n,$$

whose compact form reads as

$$B\Lambda = Q - \tilde{Q}, \tag{2.10}$$

where $Q = (Q_1, \ldots, Q_n) \in \mathbb{R}^n$, $\tilde{Q} = (\langle \phi_1, \tilde{\mathbf{u}}\rangle, \ldots, \langle \phi_n, \tilde{\mathbf{u}}\rangle) \in \mathbb{R}^n$, $\Lambda = (\lambda_1, \ldots, \lambda_n) \in \mathbb{R}^n$, and $B \in \mathbb{R}^{n\times n}$, $B_{ij} = \langle \phi_i, \mathbf{w}_j\rangle$. The matrix B is nonsingular (as will be proven in Lemma 2.3); thus, once the $\{\lambda_i\}$ are computed through relation (2.10), $(\mathbf{u}, p, \lambda_1, \ldots, \lambda_n)$ will provide a solution of (2.7).

To prove uniqueness, let $(\mathbf{u}_1, p_1, \lambda_1^{(1)}, \ldots, \lambda_n^{(1)})$ and $(\mathbf{u}_2, p_2, \lambda_1^{(2)}, \ldots, \lambda_n^{(2)})$ be two solutions of (2.7). Then

$$\begin{cases} \nu(\nabla(\mathbf{u}_1 - \mathbf{u}_2), \nabla\mathbf{v}) + \sum_{i=1}^{n} (\lambda_i^{(1)} - \lambda_i^{(2)})\langle \phi_i, \mathbf{v}\rangle - (p_1 - p_2, \operatorname{div}\mathbf{v}) = 0, \\ (q, \operatorname{div}(\mathbf{u}_1 - \mathbf{u}_2)) = 0, \\ \langle \phi_i, \mathbf{u}_1 - \mathbf{u}_2\rangle = 0, \qquad i = 1, \ldots, n, \end{cases} \tag{2.11}$$

for all $\mathbf{v} \in V$ and $q \in M$.

Taking $\mathbf{v} = \mathbf{u}_1 - \mathbf{u}_2$ in (2.11) we obtain $\nu\|\nabla(\mathbf{u}_1 - \mathbf{u}_2)\|_{L^2(\Omega)} = 0$, from which $\mathbf{u}_1 = \mathbf{u}_2$ a.e. in Ω. Consequently,

$$\sum_{i=1}^{n} (\lambda_i^{(1)} - \lambda_i^{(2)})\langle \phi_i, \mathbf{v}\rangle - (p_1 - p_2, \operatorname{div}\mathbf{v}) = 0 \qquad \forall \mathbf{v} \in V. \tag{2.12}$$

For all $i = 1, \dots, n$ we can construct $\mathbf{w}_i \in V$ which satisfy

$$\operatorname{div} \mathbf{w}_i = 0, \qquad \mathbf{w}_i|_{S_j} = 0,\ j = 1, \dots, n,\ j \neq i, \qquad \text{and} \qquad \langle \phi_i, \mathbf{w}_i \rangle = 1.$$

Note that $\langle \phi_0, \mathbf{w}_i \rangle = -1$ for all $i = 1, \dots, n$.

Taking in (2.12) $\mathbf{v} = \mathbf{w}_i$ we obtain

$$\lambda_i^{(1)} = \lambda_i^{(2)} \qquad \forall i = 1, \dots, n.$$

Finally, choosing $\mathbf{z} \in V$ such that

$$\operatorname{div} \mathbf{z} = p_1 - p_2, \qquad \mathbf{z}|_{S_i} = 0 \quad \forall i = 1, \dots, n,$$

(such a function exists; see, e.g., [9, 13]) and taking $\mathbf{v} = \mathbf{z}$ in (2.12), we obtain $\|p_1 - p_2\|_{L^2(\Omega)} = 0$. Henceforth $p_1 = p_2$ a.e. in Ω. □

LEMMA 2.3. *The matrix B introduced in* (2.10) *is nonsingular.*

Proof. Given an arbitrary vector $\boldsymbol{\alpha} \in \mathbb{R}^n$, for any $i = 1, \dots, n$ we can multiply each problem (2.9) by α_i and sum from $i = 1$ to n. Owing to the linearity of (2.9) we have

$$\text{(2.13)} \qquad \begin{cases} \nu(\sum_{i=1}^n \alpha_i \nabla \mathbf{w}_i, \nabla \mathbf{v}) - (\sum_{i=1}^n \alpha_i \pi_i, \operatorname{div} \mathbf{v}) + \sum_{i=1}^n \alpha_i \langle \phi_i, \mathbf{v} \rangle = 0, \\ (q, \operatorname{div} \sum_{i=1}^n \alpha_i \mathbf{w}_i) = 0. \end{cases}$$

Now taking in $\mathbf{v} = \sum_{i=1}^n \alpha_i \mathbf{w}_i$, we obtain

$$\nu \left\| \nabla \left(\sum_{i=1}^n \alpha_i \mathbf{w}_i \right) \right\|^2_{L^2(\Omega)} + \sum_{i=1}^n \alpha_i \left\langle \phi_i, \sum_{j=1}^n \alpha_j \mathbf{w}_j \right\rangle = 0,$$

which implies, for all $\boldsymbol{\alpha} \in \mathbb{R}^n$, $\boldsymbol{\alpha} \neq \mathbf{0}$,

$$\text{(2.14)} \qquad \boldsymbol{\alpha}^T B \boldsymbol{\alpha} = -\nu \left\| \nabla \left(\sum_{i=1}^n \alpha_i \mathbf{w}_i \right) \right\|^2_{L^2(\Omega)} \leq -\frac{\nu}{1 + C_p} \left\| \sum_{i=1}^n \alpha_i \mathbf{w}_i \right\|^2_{H^1(\Omega)} < 0.$$

In the last relation we have used the Poincaré inequality

$$\int_\Omega \mathbf{v}^2 \leq C_p \int_\Omega |\nabla \mathbf{v}|^2 \quad \forall \mathbf{v} \in V.$$

From (2.14) we infer that B is negative definite and then nonsingular. □

Remark 4. Let us point out a difficulty that may be encountered if one wants to impose on the sections S_i a mean value $P \in \mathbb{R}$ for the pressure (or, for the normal stresses) by following a route similar to that presented for the flow rate. The case where one wants to impose a pointwise value for the pressure on the boundary for the Stokes problem has been analyzed in [1]. For the sake of simplicity, we restrict ourselves to the Stokes problem. A possible formulation is as follows: find $(\mathbf{u}, p) \in V \times M$ and $\lambda_0, \dots, \lambda_n \in \mathbb{R}$ such that, for all $(\mathbf{v}, q) \in V \times M$,

$$\text{(2.15)} \qquad \begin{cases} \nu(\nabla \mathbf{u}, \nabla \mathbf{v}) + (\nabla p, \mathbf{v}) = \langle \mathbf{f}, \mathbf{v} \rangle, \\ (\nabla q, \mathbf{u}) - \displaystyle\sum_{i=0}^n \lambda_i \int_{S_i} q \, ds = 0, \\ \displaystyle\int_{S_i} p \, ds = P_i \operatorname{meas}(S_i), \quad i = 0, \dots, n. \end{cases}$$

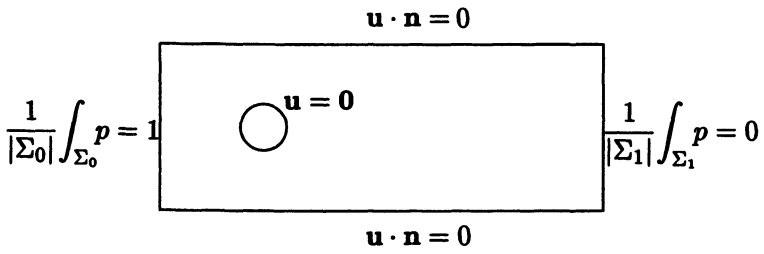

FIG. 2. *Boundary conditions for the Stokes flow around a cylinder.*

This formulation is, in some sense, the dual of the flux formulation as it imposes constraints on the dual problem (the pressure equation), whereas the flux boundary conditions yields a constraint on the primal problem (the velocity equations). Therefore, it can be regarded as the natural counterpart of our formulation for the flux problem. Unfortunately, it may be recognized that from (2.15) it follows that $\mathbf{u} \cdot \mathbf{n}|_{S_i} = \lambda_i$ on each S_i, whereas $\mathbf{u} \cdot \mathbf{n}|_{S_i}$ cannot be a constant different from 0 (since we assume no-slip boundary conditions on Γ). This formulation is therefore not unsuitable for the problem we are interested in. Nevertheless, it may be adopted in those cases where a slip boundary condition is imposed on the wall. In this case system (2.15) will effectively impose a mean value for p, thus differing from the do-nothing approach (1.5) which is instead equivalent to imposing the much stronger condition (1.6).

A numerical test is given hereafter to illustrate how the mean pressure formulation may be used when it is consistent with the velocity boundary conditions. We consider a Stokes flow around a cylinder between two flat plates. We have imposed a homogeneous Dirichlet boundary condition on the cylinder surface, a pure slip condition (i.e., $\mathbf{u} \cdot \mathbf{n} = 0$) on the plates. Moreover, we will prescribe the mean pressure at the inlet and the outlet (see Figure 2). In Figure 3 we show the pressure profile obtained at the inlet. It may be noted how it varies around the imposed mean value of 1.

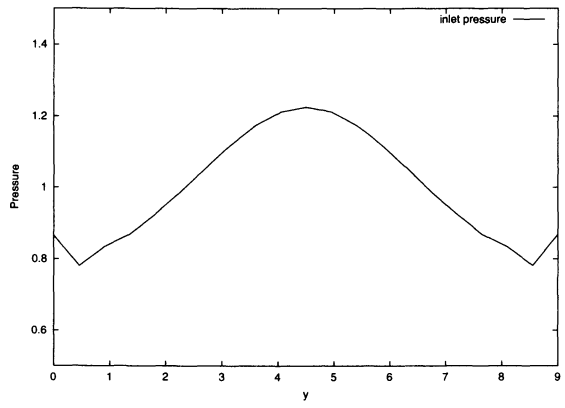

FIG. 3. *Inlet pressure distribution for the Stokes flow around a cylinder. It may be noted that the pressure is not uniform but is distributed around the imposed mean value of* 1.

3. The numerical solution of the Lagrange multipliers problem. In order to discretize formulation (2.7), we introduce a Galerkin approximation based on the finite-dimensional spaces $V_h \subset V$ and $M_h \subset M$, which we assume to satisfy the well-known LBB condition

$$\forall q_h \in M_h \quad \exists \mathbf{v}_h \in V_h,\ \mathbf{v}_h \neq 0 : \quad (q_h, \operatorname{div} \mathbf{v}_h) \geq \beta_h \|q_h\|_{L^2} \|\mathbf{v}_h\|_{H^1}. \tag{3.1}$$

Let $(\mathbf{u}_h, p_h, \lambda_{1h}, \ldots, \lambda_{nh})$ be the solution of the discrete problem. We denote by $(u_i)_{i=1\ldots dN}$ (resp., $(p_i)_{i=1\ldots M}$) the components of $\mathbf{u}_h$ (resp., p_h) with respect to a basis $\{\mathbf{v}_i\}$ of V_h (resp., $\{q_i\}$ of M_h). Finally, we introduce the vectors $U = (u_1, \ldots, u_{dN}) \in \mathbb{R}^{dN}$, $P = (p_1, \ldots, p_M) \in \mathbb{R}^M$, and $\Lambda = (\lambda_{1h}, \ldots, \lambda_{nh}) \in \mathbb{R}^n$.

Then the discrete counterpart of (2.7) gives rise to the following algebraic system of equations:

$$\begin{cases} AU + D^T P + \Phi^T \Lambda = F, \\ DU = 0, \\ \Phi U = Q, \end{cases} \tag{3.2}$$

where $A \in \mathbb{R}^{dN \times dN}$ is the stiffness matrix, $D \in \mathbb{R}^{M \times dN}$ is the matrix associated with the divergence operator, and Φ is the $n \times dN$ matrix whose lines are given by the vectors $\phi_i = (\int_{S_i} \mathbf{v}_1 \cdot \mathbf{n}\, ds, \ldots, \int_{S_i} \mathbf{v}_{dN} \cdot \mathbf{n}\, ds)$, $i = 1, \ldots, n$.

PROPOSITION 3.1. *System* (3.2) *admits a unique solution.*

Proof. The proof of the existence of the discrete solution $(\mathbf{u}_h, p_h, \lambda_{ih},\ i = 1, \ldots, n)$ as well as that of the uniqueness of $\mathbf{u}_h$ and of the λ_{ih} follows the same lines of Proposition 2.2 by substituting V and M by their discrete counterpart. The uniqueness of p_h is assured by condition (3.1). □

If we discretize in time the Navier–Stokes system (2.3) by, for instance, a semi-implicit Euler scheme and then in space by the finite element method, we will produce an algebraic system analogous to (3.2), where the matrix A is now given by

$$A = \frac{1}{\delta t} M + B + K,$$

δt being the time step, M and B the mass and advection matrices, and K the stiffness matrix. Here and in the following it is assumed that the matrix A is positive definite, which is always the case if δt is chosen appropriately.

3.1. Solution algorithms. Here, we present and analyze four possible algorithms which may be adopted for the solution of system (3.2) and which are computationally more efficient than solving simultaneously for U, P, and Λ.

1. *Solution of additional Stokes problems.* If one wishes to introduce the proposed approach on a Navier–Stokes solver with as few modifications as possible to an existing code for Navier–Stokes equations with "classical" boundary conditions, a possibility is to follow the constructive proof of Proposition 2.2. As we have seen, the solution of the constrained problem can be obtained by combining the solutions of $n + 1$ unconstrained Stokes problems, given by (2.8) and (2.9). In particular, for a fixed geometry, the n solutions $\mathbf{w}_i$, $i = 1, \ldots, n$, of problem (2.9) can be computed only once, so that the additional computational cost at each time step is just that of the solution of (2.8). The drawback is that the memory requirement to store the $\mathbf{w}_i$ may become prohibitive particularly in a three-dimensional computation and with a large number of Lagrange multipliers.

2. *Schur complement + Iterative solver.* An alternative algorithm is based on using an iterative solution of a Schur complement system. We rewrite (3.2) in the form

$$\begin{bmatrix} S & \tilde{\Phi}^T \\ \tilde{\Phi} & 0 \end{bmatrix} \cdot \begin{bmatrix} X \\ \Lambda \end{bmatrix} = \begin{bmatrix} G \\ Q \end{bmatrix}, \tag{3.3}$$

where $\tilde{\Phi} = [\Phi, 0] \in \mathbb{R}^{n \times (dN+M)}$, $X = [U, P]^T$, $G = [F, 0]^T$. The matrix

$$S = \begin{bmatrix} A & D^T \\ D & 0 \end{bmatrix}$$

has a standard Stokes form and, since the two discrete spaces V_h and M_h satisfy the LBB condition (3.1), S is nonsingular (see, e.g., [19, 2]). We can then eliminate the unknown X from (3.3), obtaining

$$\tilde{\Phi} S^{-1} \tilde{\Phi}^T \Lambda = \tilde{\Phi} S^{-1} G - Q, \tag{3.4}$$

which can be solved by an appropriate iterative method. Any matrix-vector multiplication will imply the solution of a Stokes problem with homogeneous Neumann conditions on the sections S_i.

If A is symmetric, then $R = \tilde{\Phi} S^{-1} \tilde{\Phi}^T$ is symmetric and positive definite (see Proposition 3.2 below). Consequently, the conjugate gradient (CG) algorithm may be used, which will converge to the exact solution in n iterations, n being the number of Lagrange multipliers (which coincides with the number of boundary sections S_i minus one). For instance, in the case of just one Lagrange multiplier, one iteration of the CG algorithm suffices to obtain the solution. (Note that in this case the linear system (3.4) reduces to just one scalar equation.)

Remark 5. The computational cost of the procedure depends on the number of matrix-vector multiplications required for every iteration of the chosen iterative solver and on the number of iterations necessary for convergence. For each matrix-vector multiplication we need to solve a Stokes problem. In the case of the CG algorithm, it is known that it converges to the exact solution in n steps. In addition, two extra Stokes problems have to be solved to obtain the initial residual (required to start up the procedure) and the final solution X. Therefore, if CG is adopted the computational cost would be equal to the solution of $n + 2$ Stokes problems (at each time step), which is higher than that of procedure 1. On the other hand, there is no need to store intermediate solutions.

PROPOSITION 3.2. *The matrix $R = \tilde{\Phi} S^{-1} \tilde{\Phi}^T$ is positive semidefinite; moreover, if A is symmetric, then R is symmetric and positive definite.*

Proof. System (3.3) (which is equivalent to system (3.2)) admits a unique solution, as shown in Proposition 3.1. Then, we necessarily have that $\ker(\tilde{\Phi}^T) = \{0\}$.

The matrix

$$S^* = \begin{bmatrix} A & D^T \\ -D & 0 \end{bmatrix}$$

is positive semidefinite (see, e.g., [19]), thus S^{*-1} and $R^* = \tilde{\Phi} S^{*-1} \tilde{\Phi}^T$ are also positive semidefinite.

On the other hand, $S = PS^*$, where

$$P = \begin{bmatrix} I & 0 \\ 0 & -I \end{bmatrix},$$

is such that $P^{-1} = P$. Then

$$R = \tilde{\Phi} S^{-1} \tilde{\Phi}^T = \tilde{\Phi} (P S^*)^{-1} \tilde{\Phi}^T = \tilde{\Phi} S^{*-1} P \tilde{\Phi}^T = \tilde{\Phi} S^{*-1} \tilde{\Phi}^T = R^*.$$

We conclude that also R is positive semidefinite. Moreover, if A is symmetric, R turns out to be symmetric, positive semidefinite, and nonsingular, so it is also positive definite. □

In the case where there is just one Lagrange multiplier (which occurs whenever we have just one input section and one output section), the CG algorithm reads as follows:

given $\lambda_0 \in \mathbb{R}$,

(i) $SX_1 = G - \tilde{\Phi}^T \lambda_0,$

(ii) $r_0 = \tilde{\Phi} X_1 - Q,$

(iii) $SX_2 = \tilde{\Phi}^T r_0,$

(iv) $\lambda = \lambda_0 + \dfrac{r_0^2}{r_0 \tilde{\Phi} X_2} r_0 = \lambda_0 + \dfrac{r_0^2}{\tilde{\Phi} X_2},$

(v) $SX = G - \tilde{\Phi}^T \lambda.$

Since in this case the CG method converges in one iteration, λ and X are the solutions of (3.3). This algorithm requires the solution of 3 Stokes problems at steps (i), (iii), and (v).

Remark 6. By a closer inspection, it can be noted that by taking $\lambda_0 = 0$, the CG algorithm just presented effectively reduces to procedure 1.

3. *Reordering + fractional step* I. We recall that any Stokes system of the form

$$\begin{bmatrix} A & D^T \\ D & 0 \end{bmatrix} \begin{bmatrix} U \\ P \end{bmatrix} = \begin{bmatrix} F \\ 0 \end{bmatrix}$$

can be solved exactly by the following three step algorithm:

(i) $AU_0 = F,$
(ii) $DA^{-1}D^T P = DU_0,$
(iii) $U = U_0 - A^{-1} D^T P.$

Let $H^{(1)}$ and $H^{(2)}$ denote two suitable approximations of A^{-1}. We can write an approximate factorization scheme as

(i) $AU_0 = F,$
(ii) $DH^{(1)}D^T P = DU_0,$
(iii) $U = U_0 - H^{(2)} D^T P.$

In this way we can recover many projection or quasi-compressibility methods for the Navier–Stokes equations (see [14, 17]). In particular, we will focus on the Yosida projection scheme [16], which consists of adopting $H^{(1)} = \delta t M^{-1}$ (while no approximation is made in step (iii), i.e., $H^{(2)} = A^{-1}$), and on the algebraic version of the Chorin–Temam scheme in which we have $H^{(1)} = H^{(2)} = \delta t M^{-1}$ [17].

System (3.2) can be reordered in a Stokes-like form as

$$\begin{bmatrix} \tilde{A} & \tilde{D}^T \\ \tilde{D} & 0 \end{bmatrix} \begin{bmatrix} \tilde{U} \\ P \end{bmatrix} = \begin{bmatrix} \tilde{F} \\ 0 \end{bmatrix}, \tag{3.5}$$

where

$$\tilde{A} = \begin{bmatrix} A & \Phi^T \\ \Phi & 0 \end{bmatrix} \in \mathbb{R}^{(dN+n)\times(dN+n)}, \qquad \tilde{D} = \begin{bmatrix} D & 0 \end{bmatrix} \in \mathbb{R}^{M\times(dN+n)},$$

$$\tilde{U} = \begin{bmatrix} U \\ \Lambda \end{bmatrix} \in \mathbb{R}^{dN+n}, \qquad \tilde{F} = \begin{bmatrix} F \\ Q \end{bmatrix} \in \mathbb{R}^{dN+n}.$$

We can then write an approximate factorization scheme as follows:

(i) $\tilde{A}\tilde{U}_0 = \tilde{F}$. Since A is positive definite and $\ker(\Phi^T) = \emptyset$, $\tilde{A}$ is nonsingular, too, and this system admits a unique solution. In particular, we have $\Phi U_0 = Q$.

(ii) $\tilde{D}\tilde{H}^{(1)}\tilde{D}^T P = \tilde{D}\tilde{U}_0$,

(iii) $\tilde{U} = \tilde{U}_0 - \tilde{H}^{(2)}\tilde{D}^T P$, where now $\tilde{H}^{(1)}$ and $\tilde{H}^{(2)}$ are possible approximations of $\tilde{A}^{-1}$.

We are now in the same setting of factorization schemes for the Stokes problem. We will then use the term *Yosida* scheme when $\tilde{A}^{-1}$ is approximated only in step (ii), while a scheme where $\tilde{H}^{(1)} = \tilde{H}^{(2)} \neq \tilde{A}^{-1}$ will be called a *Chorin–Temam* scheme.

We now detail a possible way to approximate $\tilde{A}^{-1}$. First, we note that if we write $\tilde{H}^{(1)}$ in the block form

$$\tilde{H}^{(1)} = \begin{bmatrix} H_{11}^{(1)} & H_{12}^{(1)} \\ H_{21}^{(1)} & H_{22}^{(1)} \end{bmatrix},$$

step (ii) of the algorithm is equivalent to

$$DH_{11}^{(1)}D^T P = DU_0,$$

where just the first diagonal block of $\tilde{H}^{(1)}$ is actually involved in the computation. Therefore, we need only look for an approximation $H_{11}^{(1)}$ of the corresponding term C_{11} of the following block decomposition of $\tilde{A}^{-1}$:

$$\tilde{A}^{-1} = \begin{bmatrix} C_{11} & C_{12} \\ C_{21} & C_{22} \end{bmatrix}.$$

The term C_{11} is equal to

$$C_{11} = A^{-1}\left(I - \Phi^T V^{-1}\Phi A^{-1}\right), \quad \text{where } V = \Phi A^{-1}\Phi^T.$$

A natural approximation of C_{11} is then

$$H_{11}^{(1)} = \delta t M^{-1}\left(I - \delta t \Phi^T V_{appr}^{-1}\Phi M^{-1}\right), \quad V_{appr} = \delta t \Phi M^{-1}\Phi^T, \tag{3.6}$$

and in particular we have $H_{11}^{(1)} = C_{11} + O(\delta t^2)$. The matrix V_{appr} is an $n \times n$ matrix. In general, the number n of Lagrange multipliers is very small so that V_{appr} can be easily inverted. Furthermore, if the lumped form of the mass matrix is used, V_{appr} is diagonal. In the case of just one Lagrange multiplier, V_{appr} reduces to a scalar.

The Yosida scheme then becomes

(i) $\tilde{A}\tilde{U}_0 = \tilde{F}$,

(ii) $DH_{11}^{(1)}D^T P = DU_0$, and

(iii) $\tilde{A}\tilde{U} = \tilde{A}\tilde{U}_0 - \tilde{D}^T P$.

We observe that, in this case, we recover exactly the constraints on the fluxes. Indeed, step (iii) implies $\Phi U = \Phi U_0 = Q$ in particular.

In the Chorin–Temam case, we note that step (iii) is equivalent to

$$U = U_0 - H_{11}^{(1)} D^T P, \tag{3.7}$$

$$\Lambda = \Lambda_0 - H_{21}^{(1)} D^T P. \tag{3.8}$$

Since we are interested only in the velocity field, we can neglect (3.8) and we need only compute the block $H_{11}^{(1)}$ as in (3.6). The algebraic Chorin–Temam scheme then becomes

(i) $\tilde{A}\tilde{U}_0 = \tilde{F}$,
(ii) $DH_{11}^{(1)} D^T P = DU_0$, and
(iii) $U = U_0 - H_{11}^{(1)} D^T P$.

We observe that, also in this case, the constraints on the fluxes are recovered exactly. Indeed, by multiplying step (iii) by Φ we have

$$\begin{aligned} \Phi U &= \Phi U_0 - \Phi H_{11}^{(1)} D^T P \\ &= \Phi U_0 - \left(\delta t \Phi M^{-1} - \delta t V_{appr} V_{appr}^{-1} \Phi M^{-1}\right) D^T P = \Phi U_0 = Q. \end{aligned}$$

4. *Reordering + fractional step* II. System (3.2) can also be reordered in a different manner as

$$\begin{bmatrix} A & \tilde{D}^T \\ \tilde{D} & 0 \end{bmatrix} \begin{bmatrix} U \\ \tilde{P} \end{bmatrix} = \begin{bmatrix} F \\ \tilde{Q} \end{bmatrix}, \tag{3.9}$$

where

$$\tilde{D} = \begin{bmatrix} D \\ \Phi \end{bmatrix} \in \mathbb{R}^{(M+n)\times dN}, \qquad \tilde{P} = \begin{bmatrix} P \\ \Lambda \end{bmatrix} \in \mathbb{R}^{M+n}, \qquad \tilde{Q} = \begin{bmatrix} 0 \\ Q \end{bmatrix} \in \mathbb{R}^{M+n}.$$

The three step algorithm then reads as

(i) $AU_0 = F$, which is unperturbed with respect to the Stokes system without constraints,
(ii) $\tilde{D}H^{(1)}\tilde{D}^T\tilde{P} = \tilde{D}U_0 - \tilde{Q}$,
(iii) $U = U_0 - H^{(2)}\tilde{D}^T\tilde{P}$.

Again, we consider the approximation $H^{(1)} = \delta t M^{-1}$ and either $H^{(2)} = A^{-1}$ (Yosida) or $H^{(2)} = \delta t M^{-1}$ (algebraic Chorin–Temam).

Remark 7. This algorithm can be easily implemented starting from an existing Navier–Stokes solver which uses factorization methods. It suffices to add to the matrix D the few lines of matrix Φ and apply the chosen factorization method.

Remark 8. Step (ii) is equivalent to

$$DH^{(1)}(D^T P + \Phi^T \Lambda) = DU_0, \tag{3.10}$$

$$\Phi H^{(1)}(D^T P + \Phi^T \Lambda) = \Phi U_0 - Q. \tag{3.11}$$

On the other hand, the third step gives

$$U = U_0 - H^{(2)}(D^T P + \Phi^T \Lambda),$$

from which we can infer that

$$\begin{aligned} \Phi U &= \Phi U_0 - \Phi H^{(2)}(D^T P + \Phi^T \Lambda) \\ &= \Phi U_0 - \Phi H^{(1)}(D^T P + \Phi^T \Lambda) + \Phi(H^{(1)} - H^{(2)})(D^T P + \Phi^T \Lambda). \end{aligned} \tag{3.12}$$

By exploiting (3.11), we finally have

$$\Phi U = Q + \Phi(H^{(1)} - H^{(2)})(D^T P + \Phi^T \Lambda). \tag{3.13}$$

Whenever $H^{(1)} = H^{(2)}$, like in the algebraic Chorin–Temam scheme, we recover the constraint on the fluxes exactly.

On the contrary, in the Yosida scheme, (3.13) becomes

$$\Phi U = Q + \Phi(\delta t M^{-1} - A^{-1})(D^T P + \Phi^T \Lambda) = Q + O(\delta t^2).$$

4. Numerical tests and algorithm assessment.

4.1. Womersley flow. In order to assess the proposed methodology, we consider a case where the analytical solution of the Navier–Stokes equations is known. More precisely, we consider the *Womersley* solution, which describes the transient flow in a cylindrical pipe associated to a time-periodic pressure gradient (see, e.g., [12]). As such, it may be considered as a transient counterpart of the Poiseuille solution.

If the pressure gradient is given by

$$\nabla p = \frac{dp}{dz}(t)\mathbf{e}_z = -\rho a \sin(\omega t)\mathbf{e}_z,$$

z being the pipe axial coordinate and ρ the fluid density, the velocity $\mathbf{u}$ reduces only to its axial component, i.e., $\mathbf{u} = u_z \mathbf{e}_z$, and the analytical expression for u_z is as follows:

- In the *two-dimensional* (2D) *case* (flow between two infinite planes),

$$u_z(r,t) = \sum_0^\infty \gamma_{2k+1} \sin\left(\frac{(2k+1)\pi}{2r_0} r\right),$$

where

$$\gamma_l = \frac{4a}{\pi l(l^4\sigma^2 + \omega^2)}\left(l^2\sigma \sin(\omega t) + \omega e^{-l^2\sigma t} - \omega\cos(\omega t)\right).$$

Here $\sigma = \frac{\mu\pi^2}{4\rho r_0^2}$, r is the transverse coordinate, $2r_0$ the distance between the two planes, and μ the dynamic fluid viscosity.

- In the *three-dimensional* (3D) *case* (flow in a cylindrical pipe),

$$u_z(r,t) = \mathrm{Re}\left\{-\frac{a}{\omega}\left(1 - \frac{J_0\left(i^{3/2}\sqrt{\frac{\rho\omega}{\mu}}r\right)}{J_0\left(i^{3/2}\sqrt{\frac{\rho\omega}{\mu}}r_0\right)}\right) e^{i\omega t}\right\},$$

where r is the radial coordinate, r_0 the cylinder radius, and J_0 the Bessel function of first kind and of order zero.

In both the 2D and 3D test cases, we have imposed homogeneous Neumann boundary conditions at the inflow, while at the outflow we have prescribed the flow rate associated to the Womersley solution. In Figure 4 we show the axial velocity field for the 2D case at two different times, together with the velocity profile at the inflow. The solution obtained agrees very well with the analytical Womersley solution. Therefore, a single condition on the flow rate at the outflow, imposed through a Lagrange multiplier, is sufficient to recover the Womersley flow.

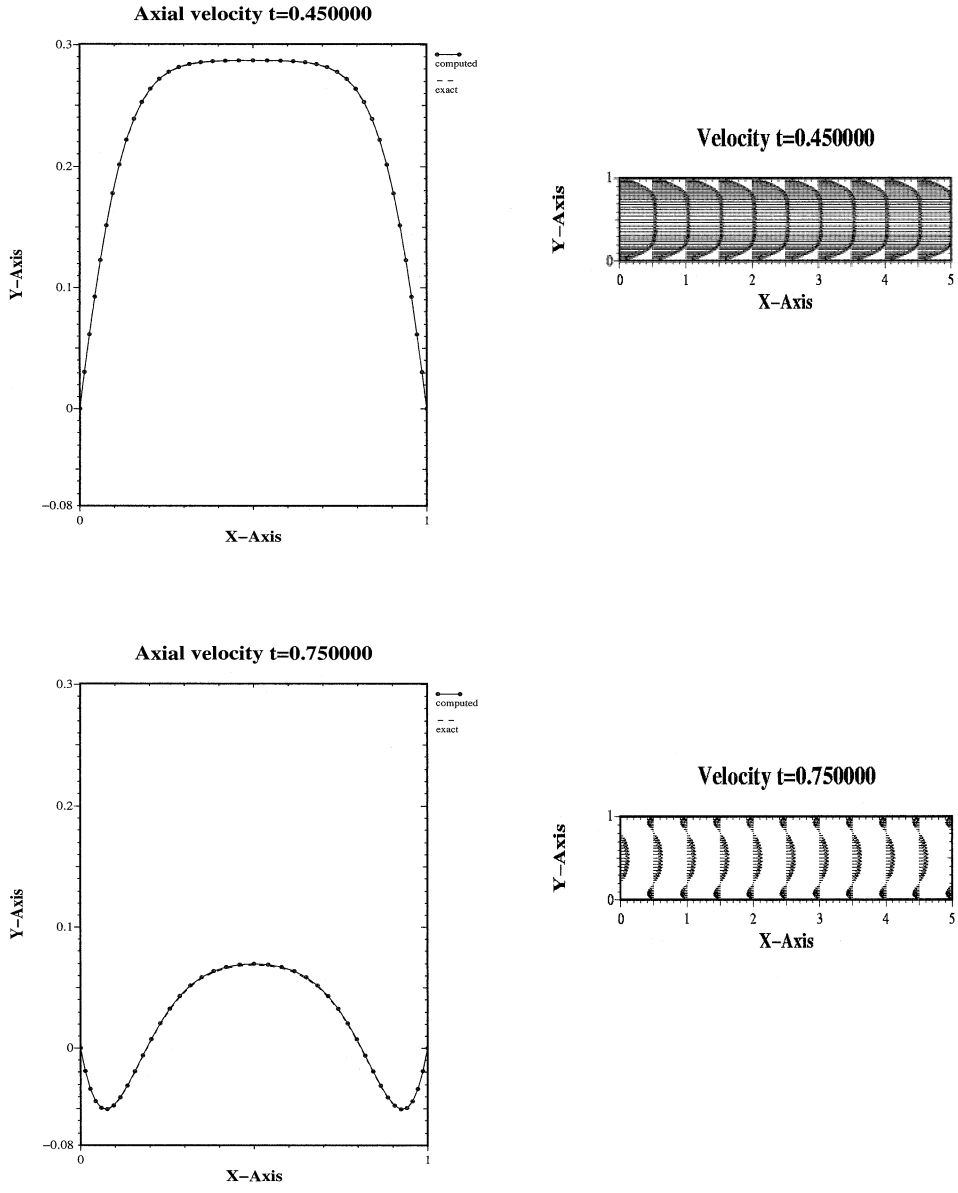

FIG. 4. *2D numerical solution obtained imposing the flux of the Womersley solution at the outflow section.*

The same experiment has been carried out in 3D and the result is shown in Figure 5. Here, the computed velocity field at three different times is illustrated, together with the corresponding axial velocity profile on the inflow section. Again, we outline the excellent agreement with the analytical solution.

Finally, we have carried out the same experiment in 2D using the numerical schemes "reordering + fractional step I" and "reordering + fractional step II" proposed in the previous section, both for the Yosida and the algebraic Chorin–Temam approximations, and we have evaluated the errors introduced on the fluxes. As expected, for the first scheme the difference between the flux we wish to impose and the one actually computed is of the order of the machine round-off error, both for the Yosida and the Chorin–Temam approximation.

For the latter scheme, this instead is true only when adopting the Chorin–Temam approximation. The behavior of the error on the fluxes for the Yosida approximation is shown in Figure 6. The error is decreasing with the time step size, with a convergence rate that appears to be even higher than quadratic.

4.2. Mass conservation in free interface simulations. We present here an application where it may be useful to impose the mass flow rate through a surface. We consider two immiscible and incompressible fluids, with the same viscosity, confined in a closed tank Ω and separated by a free interface (see Figure 7). We denote by $\Omega_i(t)$ and $\Sigma(t)$, for $i = 1, 2$, the domain occupied by the fluid i and the interface at time t, respectively. We adopt an arbitrary Lagrangian Eulerian (ALE) formulation [7] and we denote by $\mathbf{w}$ the domain velocity which satisfies $\mathbf{w} \cdot \mathbf{n} = \mathbf{u} \cdot \mathbf{n}$ on $\Sigma(t)$ and $\mathbf{w} \cdot \boldsymbol{\nu} = 0$ on $\partial\Omega$, where $\mathbf{n}$ denotes the normal to $\Sigma(t)$ directed from $\Omega_1(t)$ to $\Omega_2(t)$ and $\boldsymbol{\nu}$ is the outward normal on $\partial\Omega$. Because of the incompressibility and the immiscibility of the two fluids, the volume of $\Omega_1(t)$ (or equivalently $\Omega_2(t)$) must be preserved. At the continuous level, this property is satisfied. Indeed,

$$\begin{aligned} \operatorname{meas}(\Omega_1(t_2)) - \operatorname{meas}(\Omega_1(t_1)) &= \int_{t_1}^{t_2}\!\!\int_{\Sigma(t)} \mathbf{w} \cdot \mathbf{n}\, d\sigma = \int_{t_1}^{t_2}\!\!\int_{\Sigma(t)} \mathbf{u} \cdot \mathbf{n}\, d\sigma \\ &= \int_{t_1}^{t_2}\!\!\int_{\Omega_1(t)} \operatorname{div} \mathbf{u}\, dx = 0, \end{aligned} \tag{4.1}$$

since $\operatorname{div} \mathbf{u}$ vanishes almost everywhere in $\Omega_1(t)$.

At the discrete level, the relation $\int_{\Omega_1(t)} \operatorname{div} \mathbf{u}_h\, dx = 0$ is still verified if the pressure is discretized using *discontinuous* functions (as in the Q2/P1 or Q1/P0 finite elements) [2].

If instead the pressure is discretized using continuous functions, as in Taylor–Hood (P2/P1 or Q2/Q1), P1-isoP2, or Q1/Q1 stabilized finite elements [2, 9], there is no guarantee that (4.1) still holds at the discrete level. Numerical tests indeed confirm that those discretizations fail to conserve the measure of $\Omega_1(t)$. A possible strategy for the solution of this problem is to impose the condition

$$\int_{\Sigma(t)} \mathbf{u}_h \cdot \mathbf{n}_h\, d\sigma = 0$$

by a Lagrange multiplier, using the techniques presented in the previous section.

Let us show the results obtained on a 2D test case. In the following, all quantities are given in International System (IS) units. The two fluids are initially at rest and they are subjected to an oscillating body force $\mathbf{f} = (a\, g \sin(2\pi\nu\, t), -g)$ with $a = 0.05$,

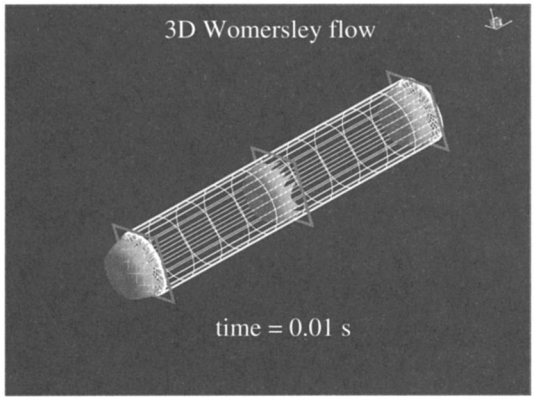

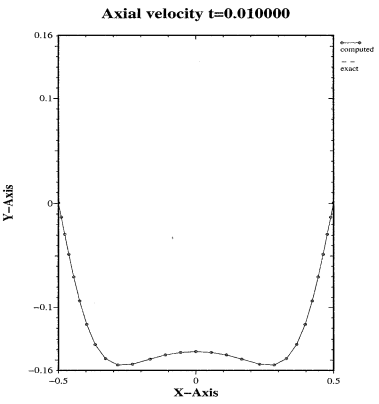

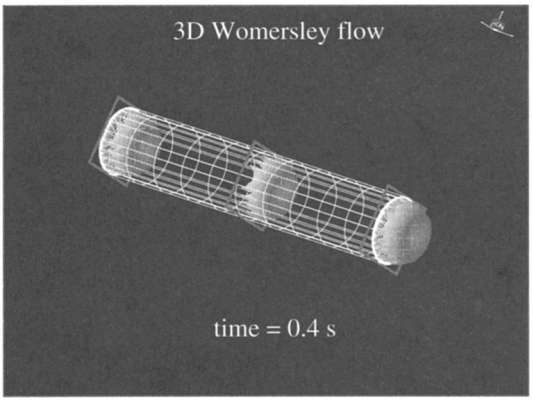

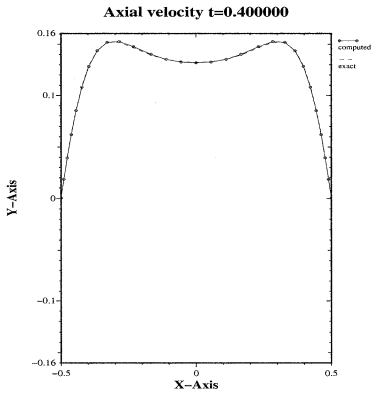

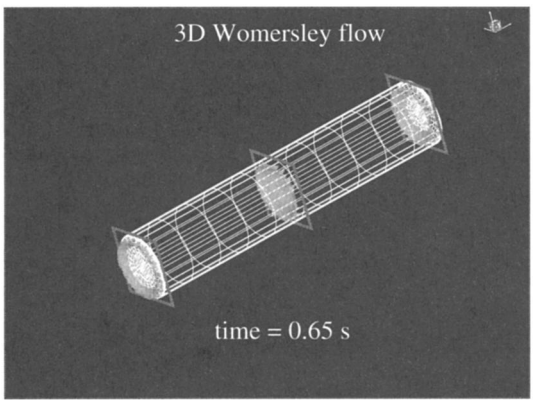

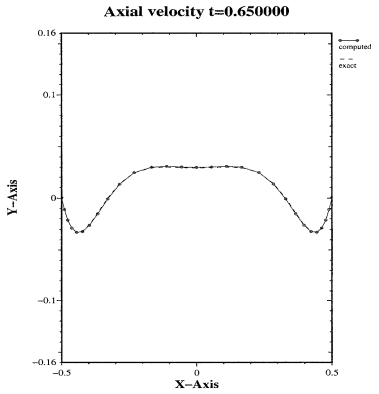

FIG. 5. *3D numerical solution obtained imposing the flux of the Womersley solution at the outflow section.*

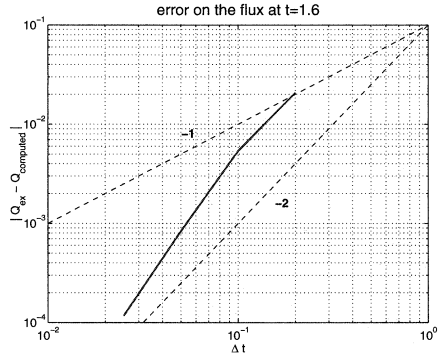

FIG. 6. *Behavior of the error on the flux for the scheme "reordering + fractional step* II*" with the Yosida approximation; the dotted lines are the reference lines for the error decrease rate.*

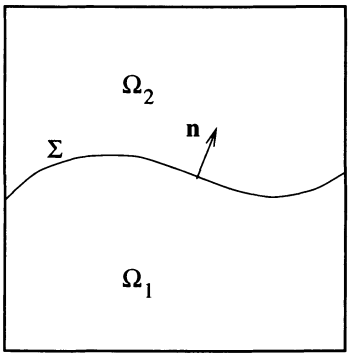

FIG. 7. *Two fluids separated by a free interface.*

$g = 10$, $\nu = 0.0625$. The kinematic viscosity of both fluids is taken to be $\nu = 0.005$, the density of the upper and the lower fluid is 0.91 and 1, respectively, $\text{meas}(\Omega_1) = \text{meas}(\Omega_2) = 4$ at $t = 0$. The mesh is allowed to move only along the vertical direction and the typical size of the mesh elements is $h = 0.1$. At time $t = 220$, if we use Q1/P0 or Q2/P1 elements, $\text{meas}(\Omega_1)$ is still equal to 4 (within machine precision), whereas it drops to approximately 3.9 when we adopt Q2/Q1 elements (see Figure 8). We have obtained analogous results with stabilized Q1/Q1 finite elements. Clearly, this lack of mass conservation decreases as h goes to zero, yet for many practical applications a mass loss is not acceptable and the use of an extremely fine mesh is not economical (or even not feasible).

Figure 8 shows that a perfect mass conservation is also obtained with Q2/Q1 elements if we impose a zero flow rate through Σ by the Lagrange multiplier technique. Finally, Figure 9 shows the elevation of a point on the interface obtained on the same mesh with the Q2/P1 elements and the Q2/Q1 elements with flux constraint. The difference is barely visible. The use of a Lagrange multiplier technique thus allows to adopt continuous pressure elements for this type of problem.

4.3. Multiscale domain decomposition. An application in which it is necessary to impose defective boundary conditions to a Navier–Stokes problem arises in the hemodynamics context when the cardiovascular system is simulated by a multiscale model. A multiscale technique couples detailed models, based on the solution

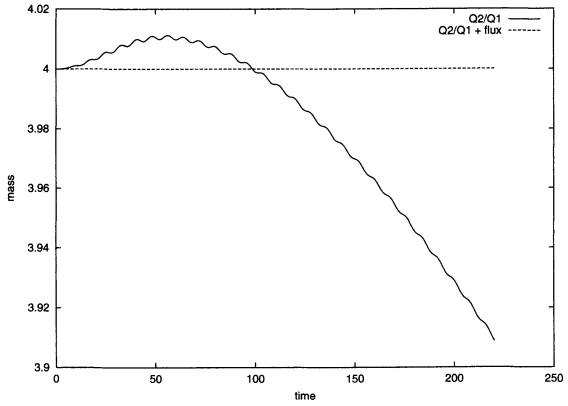

FIG. 8. *Mass conservation fails using $Q2/Q1$ elements, while it holds if we add a constraint on the velocity flux.*

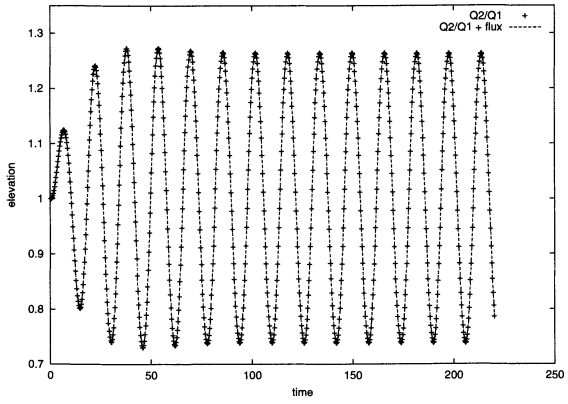

FIG. 9. *The time history of the elevation of a point of the interface. The results obtained with $Q2/P1$ elements are almost the same of that given by $Q2/Q1$ elements with flux constraint.*

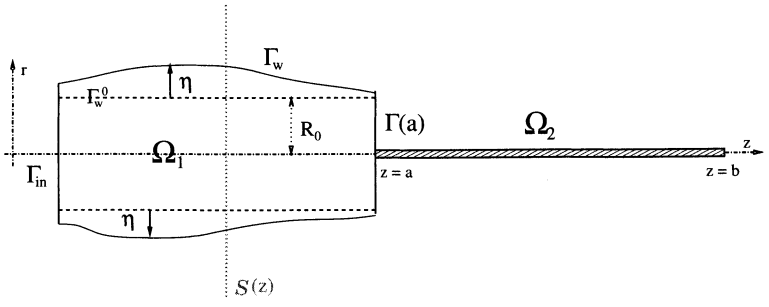

FIG. 10. *Coupled 2D-1D problem. On the left, the 2D model (Ω_1), where Γ_w represents the arterial wall and η the wall displacement with respect to the reference configuration Γ_w^0. On the right, the 1D model (Ω_2) defined on the interval $a \leq z \leq b$.*

of 2D or 3D fluid-structure interaction problems, with reduced models based on one-dimensional (1D) approximations or on systems of ordinary differential equations [8]. The simpler models normally provide the evolution of mean pressure and mean velocity in various regions of the cardiovascular system. The boundary data for the detailed model, which is based on the solution of the Navier–Stokes equations coupled with the vessel wall dynamics, must be obtained from these averaged quantities. This is a typical case of defective boundary conditions.

4.3.1. A 2D-1D coupling. Here we will give an illustrative example which consists in the coupling of a 2D and a 1D model. Let us consider the domain illustrated in Figure 10. In Ω_1 we define for $t > 0$ the fluid-structure model as

$$
\begin{cases}
\rho\partial_t \mathbf{u} + \rho\mathbf{u}\cdot\nabla\mathbf{u} + \nabla p - \mu\triangle\mathbf{u} = 0 & \text{in } \Omega_1,\\
\operatorname{div}\mathbf{u} = 0 & \text{in } \Omega_1,\\
\rho_w h\dfrac{\partial^2\eta}{\partial t^2} - kGh\dfrac{\partial^2\eta}{\partial z^2} + \dfrac{Eh}{1-\nu^2}\dfrac{\eta}{R_0^2} - \gamma\dfrac{\partial^3\eta}{\partial z^2\partial t} = f(t,z) & \text{on } \Gamma_w^0,\\
\partial_t\eta\,\mathbf{e}_r = \mathbf{u} & \text{on } \Gamma_w,\\
f(t,z) = \left(p\mathbf{n} - \mu\dfrac{\partial\mathbf{u}}{\partial\mathbf{n}}\right)\cdot\mathbf{e}_r\sqrt{1+\left(\dfrac{\partial\eta}{\partial z}\right)^2} & \text{on } \Gamma_w^0,
\end{cases}
\tag{4.2}
$$

where the unknowns are the fluid velocity $\mathbf{u}$, the fluid pressure p, and the wall displacement η. Here, ρ is the fluid density, h the vessel wall thickness, E the Young modulus, G the Timoshenko factor, and ρ_w the wall density. At $t = 0$ initial conditions $\mathbf{u}_0$, η_0, $\dot{\eta}_0$ are provided for the velocity, displacement, and displacement rate, respectively. We refer to [6] for a more detailed description and analysis of this problem. In Ω_2 we consider the following 1D problem for the velocity flux Q and the vessel section area A:

$$
\begin{cases}
\dfrac{\partial A}{\partial t} + \dfrac{\partial Q}{\partial z} = 0, & a < z < b,\ t > 0,\\
\dfrac{\partial Q}{\partial t} + \dfrac{\partial}{\partial z}\left(\alpha\dfrac{Q^2}{A}\right) + \dfrac{A}{\rho}\dfrac{\partial\bar{p}}{\partial z} + K_R\dfrac{Q}{A} = 0, & a < z < b,\ t > 0,
\end{cases}
\tag{4.3}
$$

with the algebraic relation $\bar{p} = \beta(A - A_0)$, A_0 being the reference area $A_0 = 2R_0$. The system is supplemented by initial conditions for A and Q at $t = 0$. This 1D reduced model is basically derived from (4.2), integrating the Navier–Stokes equations over each axial section $\mathcal{S}(z)$ and adopting a simplified version of the equation for the wall dynamics. A is the measure of $\mathcal{S}(z)$, the velocity flux is given by $Q(z) = \int_{\mathcal{S}(z)} u_z dr$, and $\bar{p}(z) = (\int_{\mathcal{S}(z)} p dr)/A(z)$; see [8] for more details.

System (4.2) has been discretized in space using P1-isoP2 finite elements for the fluid and P1 elements for the structure. For time discretization, we have adopted an ALE formulation to account for the domain movement with an implicit Euler discretization for the fluid equations and a Newmark scheme for the structure. On the other hand, system (4.3), which is hyperbolic, has been discretized using a second-order Taylor–Galerkin scheme with a characteristic treatment of the boundary.

At each time step t^n, we look for a solution of (4.2) and (4.3) which satisfies at $\Gamma(a)$ the coupling conditions

$$
\operatorname{meas}(\Gamma^n(a)) = A^n(a), \quad \int_{\Gamma^n(a)} u_z^n = Q^n(a), \quad \frac{1}{\operatorname{meas}(\Gamma^n(a))}\int_{\Gamma(a)} p^n = \bar{p}^n(a).
\tag{4.4}
$$

We have solved iteratively at each time step the two subproblems in Ω_1 and Ω_2. Given the approximate solution $\mathbf{u}^n$, p^n, η^n, Q^n, and A^n of the coupled problem at time $t = t^n$, we look for the solution $\mathbf{u}^{n+1}$, p^{n+1}, η^{n+1}, Q^{n+1}, and A^{n+1} using the following iterative algorithm:

We set $\mathbf{u}_{(0)} = \mathbf{u}^n$, $p_{(0)} = p^n$, and $\eta_{(0)} = \eta^n$, and for $k = 0, 1, \ldots$ we do the following:

1. We solve the 1D model (4.3) imposing at $z = a$

$$A_{(k+1)}(a) = A_0 + \frac{1}{\beta \,\mathrm{meas}(\Gamma_{(k)}(a))} \int_{\Gamma(a)} p_{(k)}$$

and at $z = b$ absorbing boundary conditions based on characteristic analysis. We obtain $Q_{(k+1)}$ and $A_{(k+1)}$ in Ω_2.

2. We then solve the 2D problem imposing on $\Gamma(a)$ for the Navier–Stokes equations the defective condition

$$\int_{\Gamma(a)} \mathbf{u}_{(k+1)} \cdot \mathbf{e}_z = Q_{(k+1)}(a)$$

and for the structure at $z = a$

$$\eta_{(k+1)}(a) = \frac{1}{2} A_{(k+1)}(a) - R_0.$$

We obtain $\mathbf{u}_{(k+1)}$, $p_{(k+1)}$, $\eta_{(k+1)}$ in Ω_1.

We iterate until the coupling conditions are satisfied within a fixed tolerance and we finally set the solution at time t^{n+1} equal to the converged value. We may eventually add a relaxation step on the variable $A_{(k)}(a)$.

We observe that in step 2 of this algorithm we have to solve Navier–Stokes equations with flux boundary conditions on $\Gamma(a)$. A different algorithm for the same coupled 2D/1D problem, which allows us to impose a mean pressure condition on $\Gamma(a)$, has been proposed and analyzed in [6].

We present here the numerical results relative to the following test case: we have considered a fluid initially at rest and we have imposed a pressure of $15 mmHg$ ($2{\cdot}10^4\, dynes/cm^2$) at the inlet ($\Gamma_{in}$) for 0.005 seconds. For the fluid we have taken $\mu = 0.035\, poise$ and $\rho = 1\, g/cm^3$, while for the structure we have $E = 0.75{\cdot}10^6\, dynes/cm^2$, $\nu = 0.5$, $\rho_w = 1.1\, g/cm^3$, and $h = 0.1\, cm$. Figure 11 shows the fluid pressure and the domain deformation at different times. We may note how the "pressure wave" crosses the interface between the two models with little spurious reflections.

4.3.2. A two-dimensional–zero-dimensional coupling. This time, a by-pass anastomosis in a coronary, modeled by the incompressible Navier–Stokes equations in a fixed domain, is coupled with a lumped parameter model for the rest of the cardiovascular system. Lumped parameters models are well established tools [21] and able to provide an approximation of the time evolution of average pressure and flow rate in different compartments of the cardiovascular system. They are based on the solution of a system of algebraic-ordinary differential equations derived by using an analogue with an electrical circuit. In this analogy, electrical currents and voltage are interpreted as flow rate and mean pressure, respectively. The model here adopted is the one proposed in [11]. Its coupling with a 2D description of a coronary by-pass is shown in Figure 12.

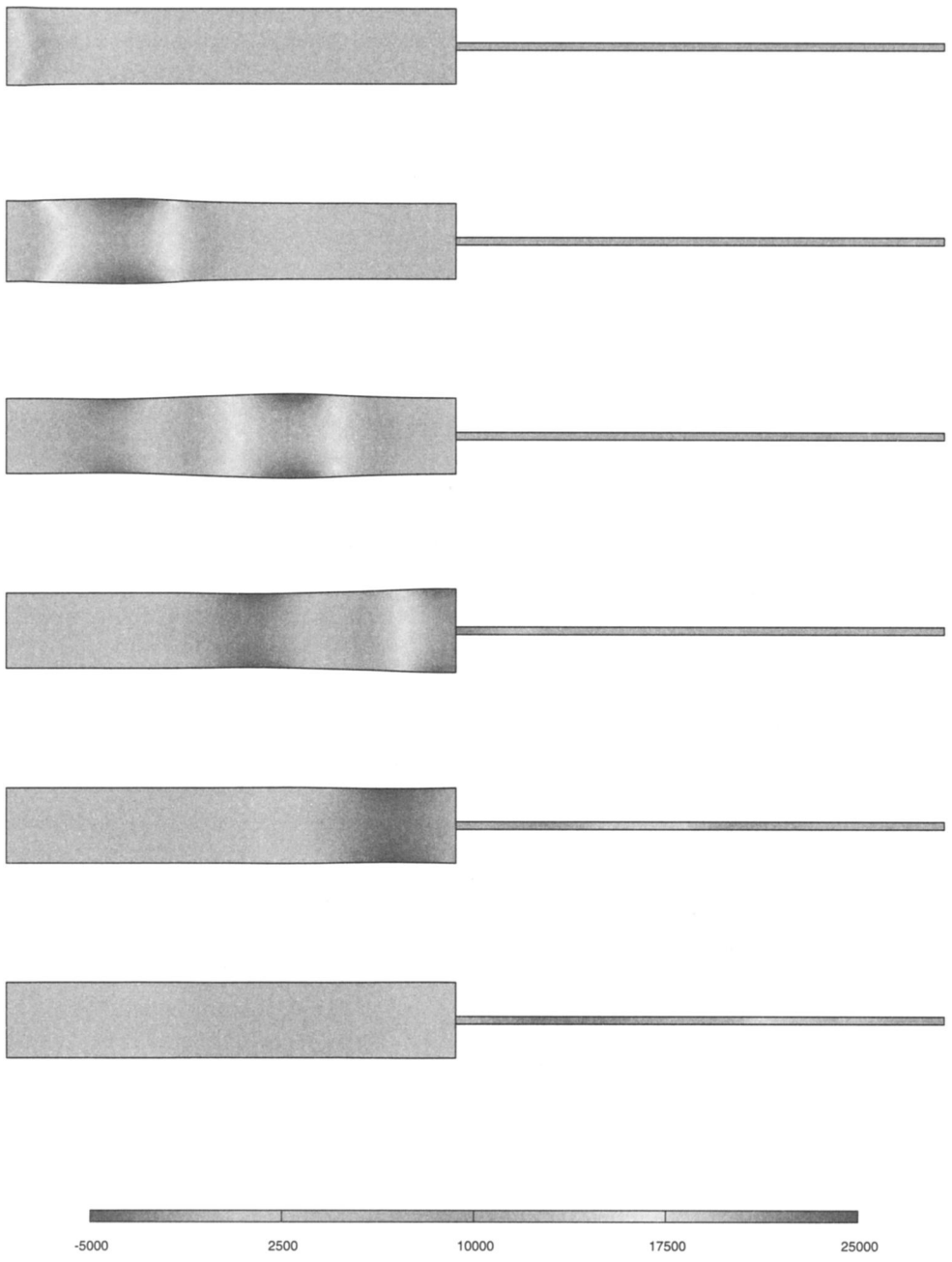

FIG. 11. *Coupling 2D simulation with the 1D reduced model; pressure distribution every 5 ms, starting from $t = 1\,ms$.*

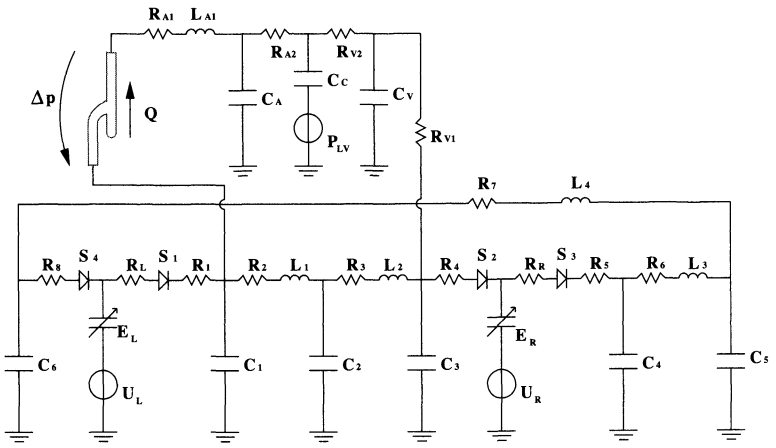

FIG. 12. *Lumped parameter model of the circulatory system coupled with a 2D description of a coronary by-pass.*

The interface condition we wish to impose between the two models are the continuity of flow rate and mean pressure. The numerical scheme employs a staggered algorithm where the pressure drop between inflow and outflow calculated by the Navier–Stokes model at a generic time step $t = t^k$ is imposed to the lumped parameter model which, in turn, is used to obtain the flow rate to advance the Navier–Stokes solution to $t = t^{k+1}$. We are therefore facing the case where we need to employ the technique presented in section 2. Since we are using a rigid wall model for the by-pass, the incoming and outgoing flow rates are equal, due to the incompressibility constraint. Actually, we have prescribed to the Navier–Stokes equations only the flow rate on the inflow section while homogeneous Neumann boundary conditions have been imposed on the outflow section. On the other hand, the pressure drop between inflow and outflow, needed to advance the lumped parameter model, is simply provided by the Lagrange multiplier.

An alternative coupling algorithm, based on imposing a mean pressure to the inflow and outflow sections of the Navier–Stokes problem while prescribing the flow rate to the lumped model, has been described in [15].

At the top of Figure 13 we show the flow rate and the pressure drop in the by-pass computed by the coupled system. The marks indicate the values at the times corresponding to the four snapshots of the fluid speed found in the lower part of the same figure.

5. Conclusions. In this work we have considered defective boundary conditions for Navier–Stokes equations. In particular, we have addressed the case where one wants to impose the flow rate on a measurable subset of the domain boundary. We have proposed a formulation based on a Lagrange multiplier technique and we have shown that it is well-posed for the Stokes and the linearized Navier–Stokes equations. Moreover, we have considered some numerical algorithms to effectively solve the mixed problem thus obtained. Finally, we have presented several applications in which the technique may be advantageously used and we have shown some numerical results illustrating its effectiveness.

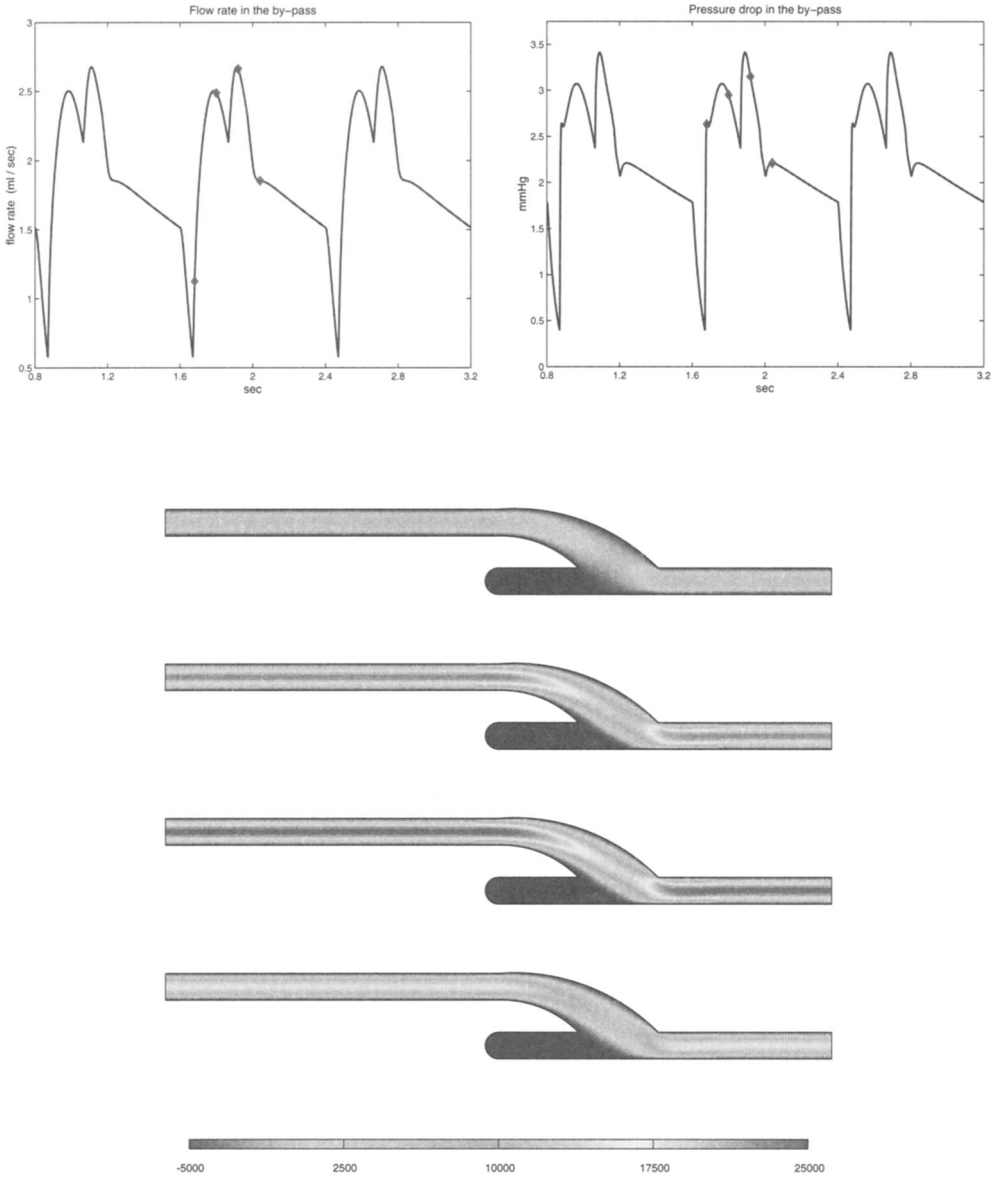

FIG. 13. *On the top: flow rate and pressure drop in the by-pass. On the bottom: fluid speed at* $t = 1.68\,s, 1.8\,s, 1.92\,s, 2.04\,s$.

REFERENCES

[1] C. BÈGUE, C. CONCA, F. MURAT, AND O. PIRONNEAU, *Les équations de Stokes et de Navier-Stokes avec des conditions aux limites sur la pression*, in Nonlinear partial differential equations and their applications, Collège de France Seminar, Vol. IX (Paris, 1985–1986), Longman Scientific and Technical, Harlow, UK, 1988, pp. 179–264.

[2] F. BREZZI AND M. FORTIN, *Mixed and Hybrid Finite Elements*, Springer Ser. Comput. Math. 15, Springer-Verlag, New York, 1991.

[3] C.H. BRUNEAU, *Boundary conditions on artificial frontiers for incompressible and compressible Navier-Stokes equations,* M2AN Math. Model. Numer. Anal., 34 (2000), pp. 303–314.

[4] C.H. BRUNEAU AND P. FABRE, *Effective downstream boundary conditions for incompresisble Navier-Stokes equations,* Internat. J. Numer. Methods Fluids, 19 (1994), pp. 693–705.

[5] C. CONCA, C. PARES, O. PIRONNEAU, AND M. THIERET, *A computational model of Navier-Stokes equations with imposed pressure and velocity fluxes,* Internat. J. Numer. Methods Fluids, 20 (1995), pp. 267–287.

[6] L. FORMAGGIA, J.-F. GERBEAU, F. NOBILE, AND A. QUARTERONI, *On the coupling of 3D and 1D Navier-Stokes equations for flow problems in compliant vessels,* Comput. Methods Appl. Mech. Engrg., 191 (2001), pp. 561–582.

[7] L. FORMAGGIA AND F. NOBILE, *A stability analysis for the arbitrary Lagrangian Eulerian formulation with finite elements,* East-West J. Numer. Math., 7 (1999), pp. 105–132.

[8] L. FORMAGGIA, F. NOBILE, A. QUARTERONI, AND A. VENEZIANI, *Multiscale Modelling of the Circulatory System: A preliminary analysis,* Comput. Vis. Science, 2 (1999), pp. 75–83.

[9] V. GIRAULT AND P.-A. RAVIART, *Navier–Stokes Equations: Theory and Numerical Analysis*, Springer Ser. Comput. Math. 5, Springer-Verlag, Berlin, 1986.

[10] J.G. HEYWOOD, R. RANNACHER, AND S. TUREK, *Artificial boundaries and flux and pressure conditions for the incompressible Navier–Stokes equations,* Internat. J. Numer. Methods Fluids, 22 (1996), pp. 325–352.

[11] F. INZOLI, F. MIGLIAVACCA, AND S. MANTERO, *Pulsatile flow in an aorto-coronary bypass 3-D model*, in Biofluid Mechanics, Proceedings of the Third International Symposium, Munich, Germany, D. Liepsch, ed., VDI Verlag, Dusseldorf, 1994.

[12] D.A. MCDONALD, *Blood Flow in Arteries*, 3rd ed., W.W. Nichols and M.F. O'Rourke, eds., Edward Arnold, London, 1990.

[13] F.C. OTTO AND G. LUBE, *A non-overlapping domain decomposition method for the Oseen equations,* Math. Models Methods Appl. Sci., 8 (1998), pp. 1091–1117.

[14] B. PEROT, *An analysis of the fractional step method,* J. Comput. Phys., 108 (1993), pp. 51–58.

[15] A. QUARTERONI, S. RAGNI, AND A. VENEZIANI, *Coupling between lumped and distributed models for blood flow problems,* Comput. Vis. Science, 4 (2001), pp. 111–124.

[16] A. QUARTERONI, F. SALERI, AND A. VENEZIANI, *The Yosida method for the numerical approximation of Navier-Stokes equations,* J. Math. Pures Appl. (9), 78 (1999), pp. 473–503.

[17] A. QUARTERONI, F. SALERI, AND A. VENEZIANI, *Factorization methods for the numerical approximation of Navier-Stokes equations,* Comput. Methods Appl. Mech. Engrg., 188 (2000), pp. 505–526.

[18] A. QUARTERONI, M. TUVERI, AND A. VENEZIANI, *Computational vascular fluid dynamics: Problems, models and methods,* Comput. Vis. Science, 2 (2000), pp. 163–197.

[19] A. QUARTERONI AND A. VALLI, *Numerical Approximation of Partial Differential Equations*, Springer Ser. Comput. Math. 23, Springer-Verlag, Berlin, 1994.

[20] R. TEMAM, *Navier-Stokes Equations. Theory and Numerical Analysis*, 3rd ed., North-Holland, Amsterdam, 1984.

[21] N. WESTERHOF, F. BOSMAN, C.D. VRIES, AND A. NOORDERGRAAF, *Analog studies of the human systemic arterial tree,* J. Biomech., 2 (1969), pp. 121–143.